

RIGID BODY TRANSLATION IN MULTISTAGE SINGLE POINT INCREMENTAL FORMING

LIN PRAKASH P S

A Dissertation Submitted to
Indian Institute of Technology Hyderabad
In Partial Fulfilment of the Requirements for
The Degree of Master of Technology




भारतीय प्रौद्योगिकी संस्थान हैदराबाद
Indian Institute of Technology Hyderabad

Department of Mechanical & Aerospace Engineering

June, 2014

Declaration

I declare that this written submission represents my ideas in my own words, and where others' ideas or words have been included, I have adequately cited and referenced the original sources. I also declare that I have adhered to all principles of academic honesty and integrity and have not misrepresented or fabricated or falsified any idea/data/fact/source in my submission. I understand that any violation of the above will be a cause for disciplinary action by the Institute and can also evoke penal action from the sources that have thus not been properly cited, or from whom proper permission has not been taken when needed.



LIN PRAKASH P.S.

ME12M1013

Approval Sheet

This thesis entitled “Rigid Body Translation in Multistage Single Point Incremental Forming” by Lin Prakash P S is approved for the degree of Master of Technology from IIT Hyderabad.



Dr. S Surya Kumar

Department of Mechanical and Aerospace Engineering

IIT Hyderabad

Internal Examiner

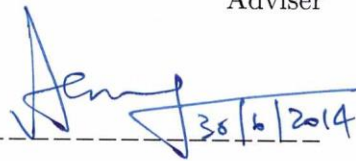


Dr. N Venkata Reddy

Department of Mechanical and Aerospace Engineering

IIT Hyderabad

Adviser



Dr. A Venugopal Rao

DMRL Hyderabad

External Examiner



Dr. Manish K Niranjana

Department of Physics IIT Hyderabad

Chairman

Acknowledgements

I would like to thank my thesis advisor Prof. N.Venkata Reddy for the support and valuable suggestions.

I thank my fellow lab mates Rakesh Lingam, Mallikarjuna Kishan, Ankush Bansal and Chhavikant Sahu for the technical support. I would like to convey my thanks to Abhishek Kumar and Shibin E. I thank my friends Jis Tom, Tony Thomas, Anwar Sadath, & Mohammed Ali for the encouragement they have given.

I would like to thank my parents who supported and stood with me at tough times.

Lin Prakash P.S.

Dedicated to My Parents

Abstract

Incremental Sheet Metal Forming (ISMF) is an innovative sheet metal forming method which uses a Computer Numerical Controlled (CNC) vertical milling machine & basic tooling. ISMF has the potential to form complex 3D parts without using specific tooling. The formability of sheet metal is better for incremental forming than in conventional sheet metal forming. Even though the formability is higher in ISMF, forming components having higher wall angles is not possible. So multistage ISMF is used in which the required component is formed with various intermediate stages. In this work, an attempt is made to calculate rigid body translation which has to be considered for avoiding stepped features. The Finite Element Analysis results of a cone component modelled in ABAQUS is analyzed which gives an idea about the deformation pattern and material flow.

Literature review indicates that it is impossible to form a vertical wall angle component in single stage Single Point Incremental Forming (SPIF). When multistage strategy is used, it resulted in the accumulation of rigid body translations which resulted in the formation of stepped features at the bottom of the component. One method to eliminate this is to use a combination of out to in & in to out tool movement in intermediate stages. Calculating the rigid body translation is an important step. Rigid body translation is calculated for given intermediate profiles to avoid formation of stepped features.

Contents

Declaration.....	ii
Approval Sheet.....	iii
Acknowledgements.....	iv
Abstract.....	vi
1 Introduction and Literature Review.....	1
1.1 Introduction.....	1
1.2 Literature Review.....	2
1.2.1 Configuration of incremental sheet metal forming process.....	2
1.2.2 Formability Studies.....	2
1.3 Objective of Present Work.....	10
1.4 Organization of the Thesis.....	10
2 Methodology.....	11
2.1 Tool Path Planning for Multi-stage.....	11
2.1.1 Tool Radius Compensation.....	12
2.2 Rigid Body Translation.....	12
3 Results.....	15
3.1 Thickness Calculation.....	15
3.1.1 Thickness Variation.....	17
3.2 Rigid Body Translation.....	21
4 Conclusions & Scope for future work.....	26
4.1 Conclusions.....	26
4.2 Scope for future work.....	26
References.....	27
Appendix.....	28

A.1	Experimental Setup.....	28
A.1.1	Specifications of the machine.....	28
A.1.2	Work zero setting.....	29
A.1.2.1	Top tool work zero setting.....	29
A.1.2.2	Bottom tool work zero setting.....	29
A.1.3	Clamping Plates.....	30
A.2	FEM (Post Processing) Analysis.....	33

Chapter 1

Introduction and Literature Review

1.1 Introduction

Sheet metal forming has various applications in automobile and aerospace industries. Conventional sheet metal forming processes requires expensive tooling which can be affordable only for mass production of components. To overcome the above mentioned problem, incremental sheet metal forming has been introduced.

Incremental sheet metal forming does not need specific tooling and dies. Incremental sheet metal forming enables three dimensional shaping of complex parts without dedicated dies.

A schematic arrangement for incremental sheet metal forming is shown in fig1.1 [1]

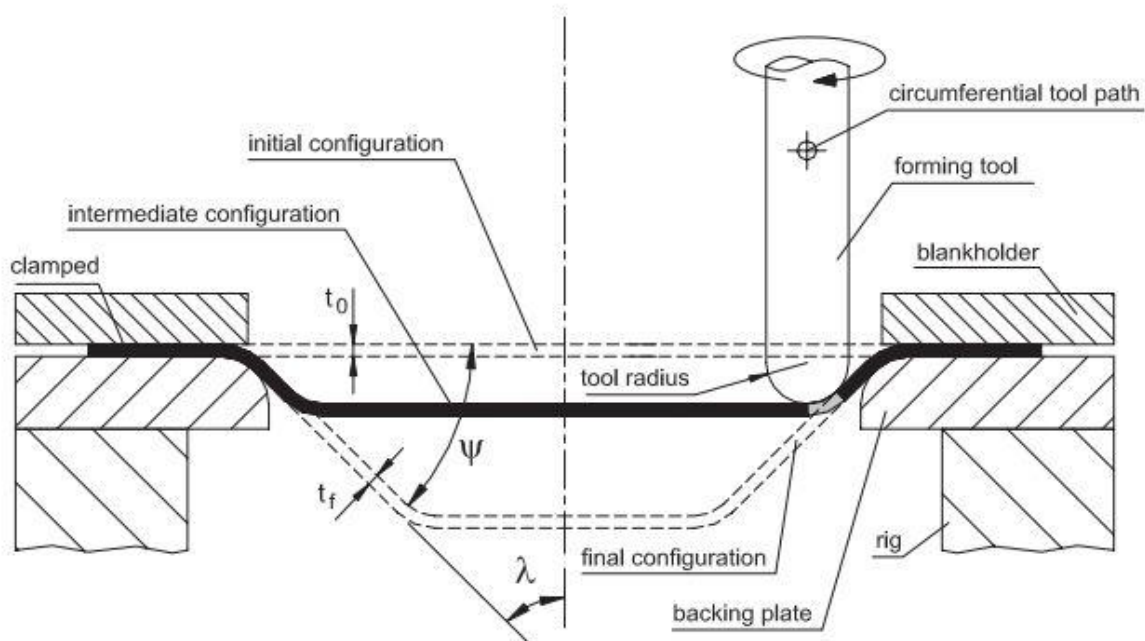


Figure 1.1: Schematic diagram of incremental sheet metal forming process [1]

In Incremental sheet metal forming, a hemispherical head tool is moved through a predetermined path 3-axis CNC machine. Sheet is being locally deformed in incremental steps during this process.

The final wall thickness (t_f) of the formed component can be predicted by using Sine law based on the initial thickness (t_0) and the wall angle (ψ).

$$t_f = t_0 \sin(90 - \psi)$$

1.2 Literature Review

1.2.1 Configuration of Incremental Sheet Metal Forming Process

Configuration for incremental forming can be classified into two viz; with and without die which can be further subdivided into negative and positive incremental forming. Negative die less forming is known as Single Point Incremental Forming (SPIF) in which there is only one forming tool. Positive die less incremental forming is known as Two Point Incremental Forming (TPIF). The four configurations of incremental forming are shown in Fig.1.2

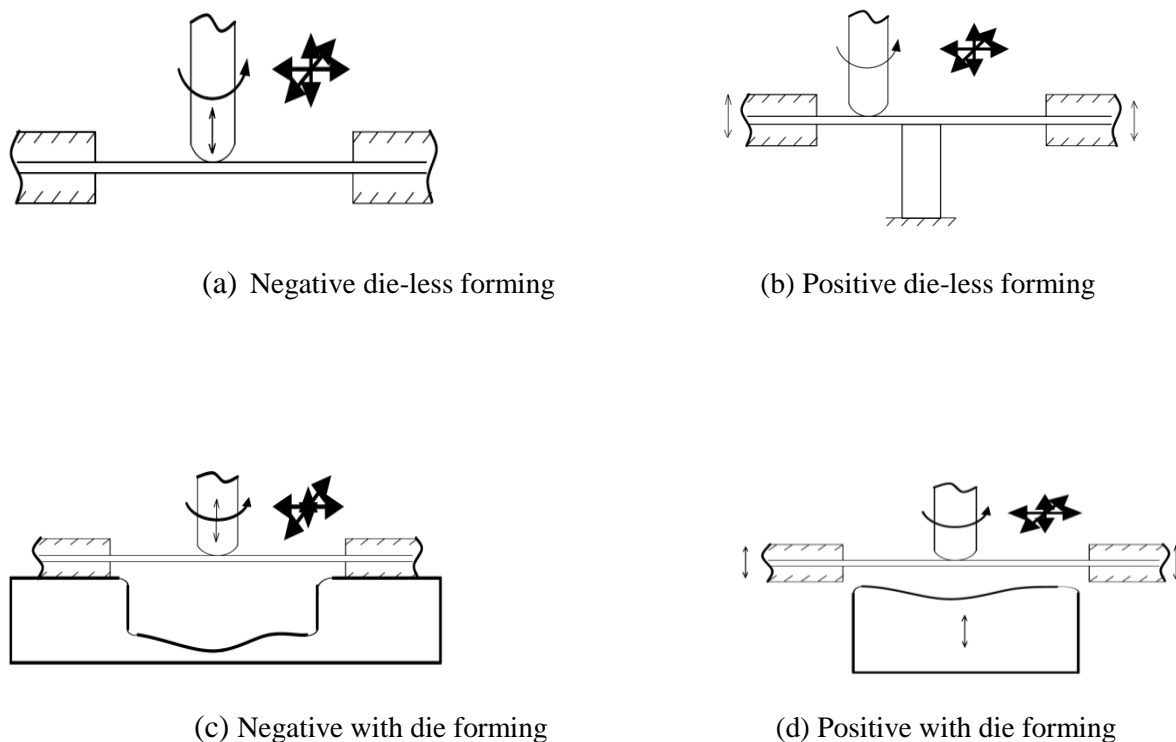


Figure 1.2: Four configurations of ISMF [2]

1.2.2 Formability Studies

Shim and Park [3] measured the major and minor strains of deformed grids. They found out that the forming limit curve is a straight line with negative slope in the positive region of the minor strain the forming limit diagram. They observed that bi-axial stretching occurs near the corners and plane strain occurs along the straight side.

Kim and Park [4] has done experiments to find the formability and showed that in negative incremental forming both plane- strain stretching mode and biaxial stretching mode of deformation are present, while in positive incremental forming only the plane-strain stretching mode is present. They concluded that with the negative incremental forming, it is difficult to form sharp corners or edges because cracks easily occur due to the biaxial mode of deformation.

Silva et al. [5] proposed a theoretical model based on membrane analysis for rotationally symmetric SPIF component. The expressions for principal stresses in meridional, circumferential and thickness directions were calculated. It has been observed that crack propagation is due to tensile meridional stresses. It has been shown that necking is suppressed in SPIF. But strain hardening and anisotropy were not considered in this study. The forming limit curve is shown in Fig.1.3. They found out that opening of cracks are due to meridional stress as shown in Fig.1.4.

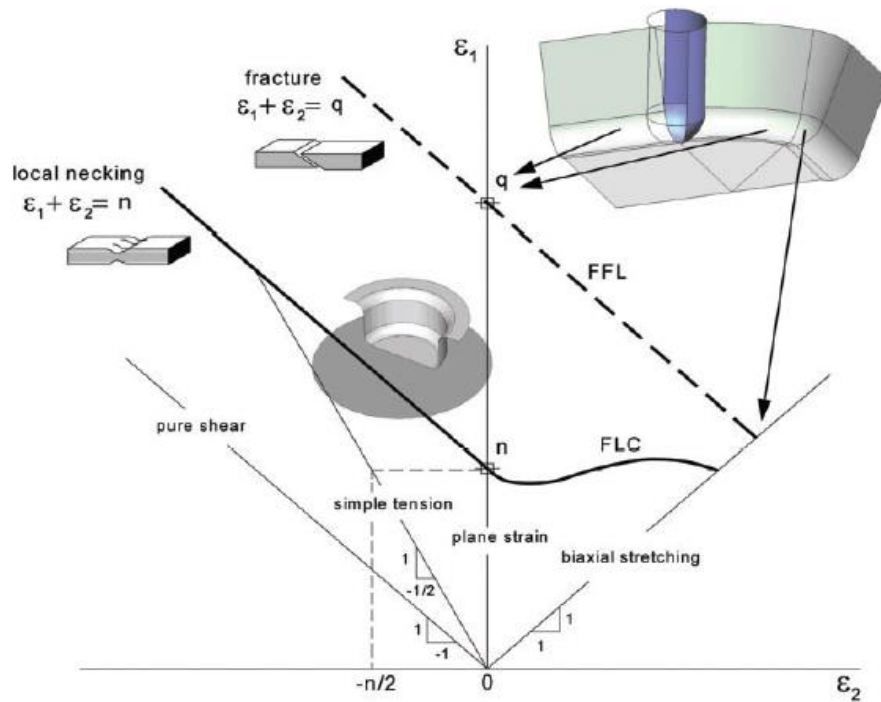


Figure 1.3: Schematic representation of the forming limit curve in the principal strain space [5]

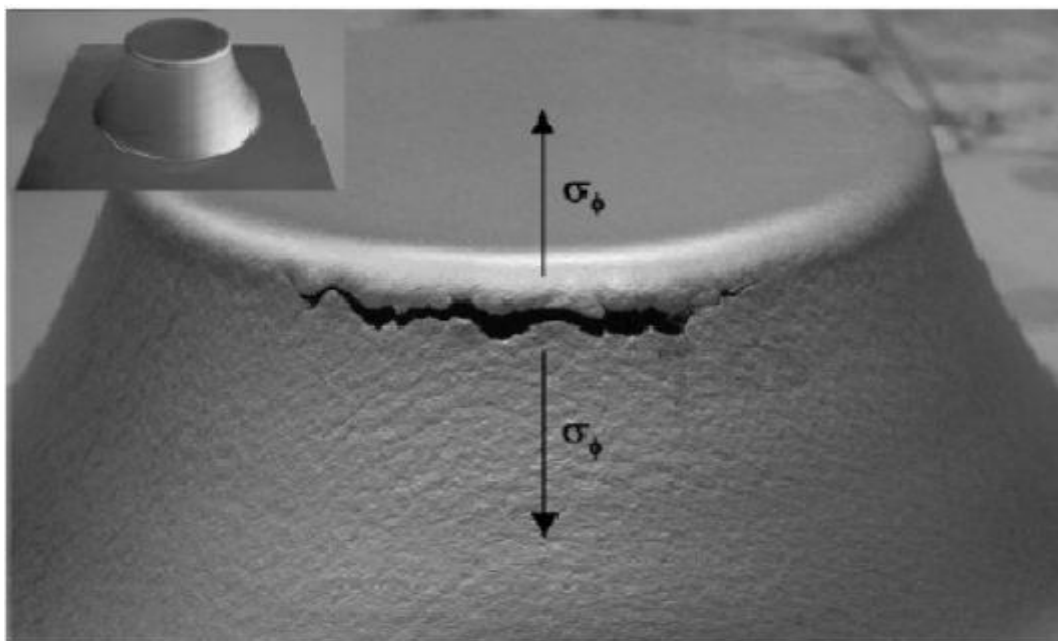


Figure 1.4: Opening of cracks due to meridional stress [5]

Filice et al. [6] studied the influence of mechanical properties of the sheet material on formability in Single point incremental forming and they found out that strain hardening coefficient has the highest influence on material formability. They concluded that material formability increases as the strain hardening coefficient increases.

Duflou et al. [7] has done experimental studies on force measurements in single point incremental forming. The effect of process parameters like tool diameter, vertical depth increment, wall angle and thickness of sheet in the force required to form the sheet metal was analysed. It has been found out that forces increases as the step size, tool diameter, wall angle and thickness increases as shown in Fig.1.5-1.8

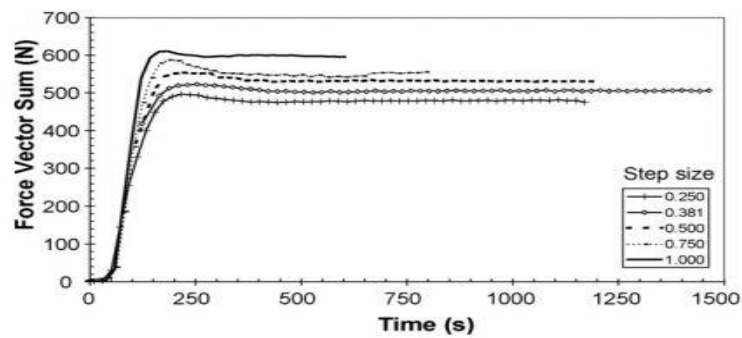


Figure 1.5: Variations of forces with step size [7]

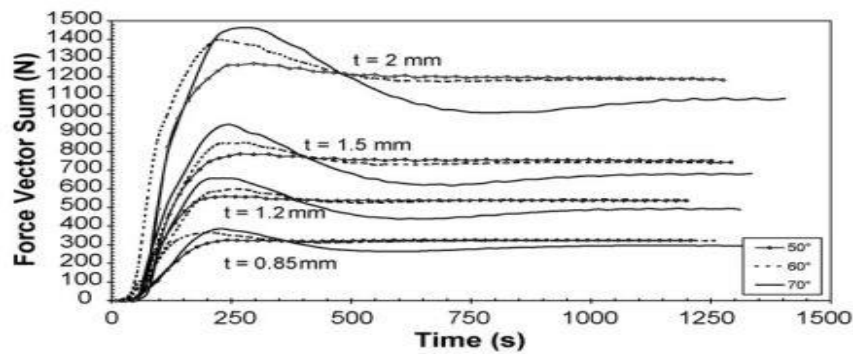


Figure 1.6: Variation of forces with thickness [7]

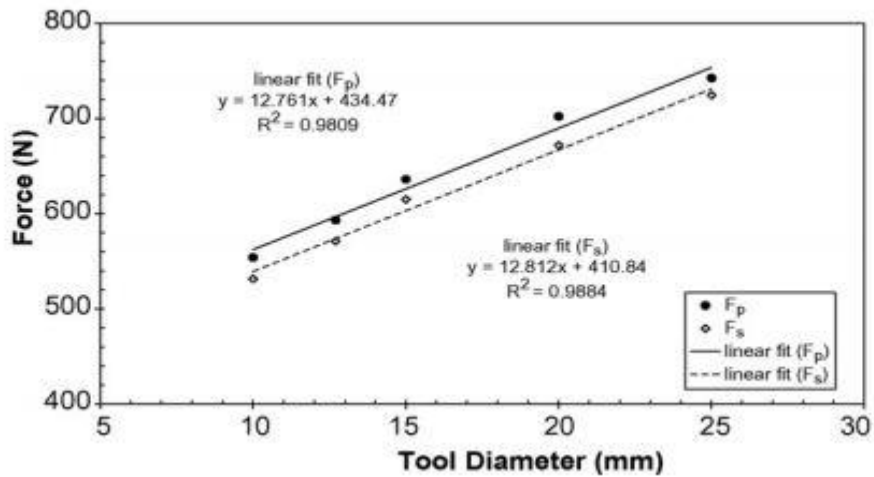


Figure 1.7: Variation of forces with tool diameter [7]

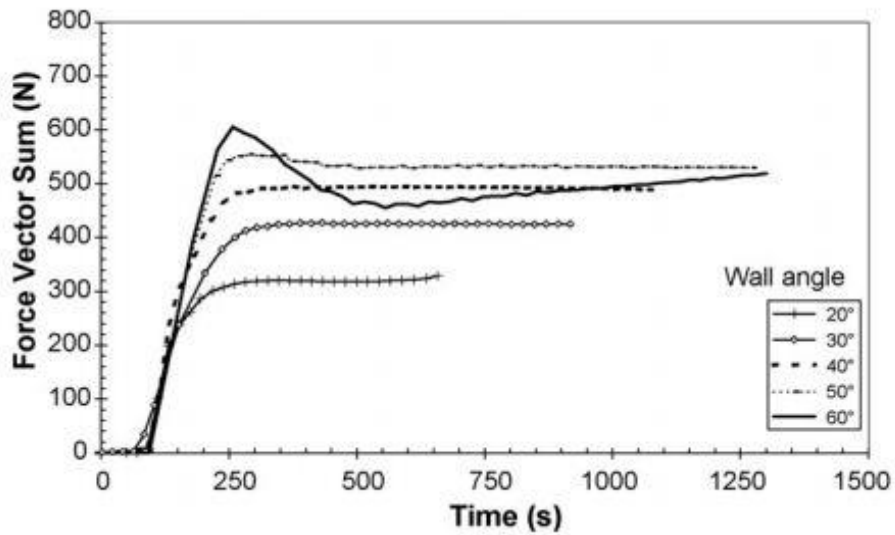


Figure 1.8: Variation of forces with wall angle [7]

Allwood et al. [8] studied the mechanism of deformation of ISMF using copper sheets. It has been observed that stretching and shear occurs in plane perpendicular to the tool movement direction shear occurs in plane parallel to tool movement direction. The major component of strain is the shear in the plane parallel to tool movement direction. It has been concluded that through thickness shear components have a significant effect in the deformation mechanism of both SPIF and TPIF.

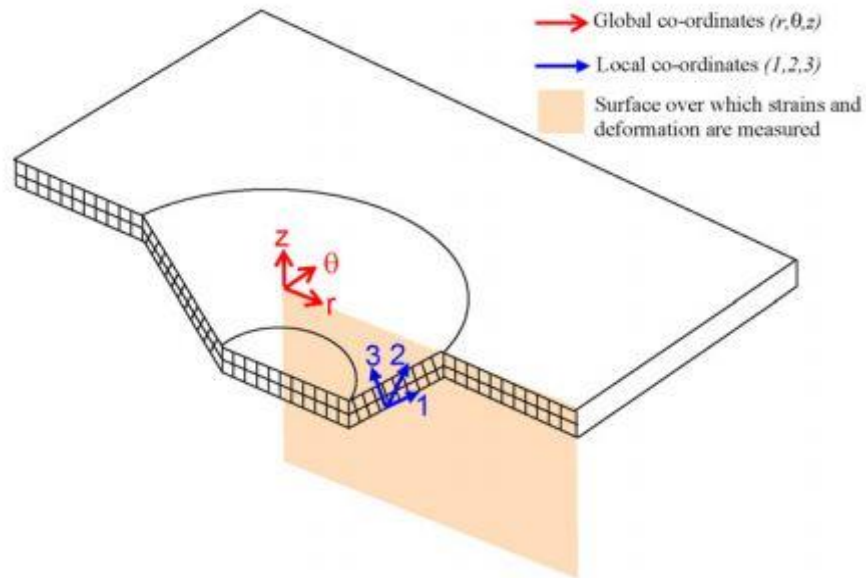


Figure 1.9: 3-D representation of global and local coordinate sets for SPIF [8]

To predict the final thickness of formed component, sine law can be used. The final wall thickness (t_f) of the formed component can be predicted by using Sine law based on the initial thickness (t_0) and the wall angle (ψ).

$$t_f = t_0 \sin(90 - \psi)$$

But for higher wall angle components, sine law is not valid because thickness become very negligible.

Jeswiet et al. [9] conducted experiments to study the wall thickness variations in single point incremental forming and they found out that the wall thickness in some specific regions is less than the sine law predicted thickness as shown in Fig.1.10. So material redistribution is needed from regions having more thickness to those regions where excessive thinning takes place. To achieve this, multistage strategy is proposed.

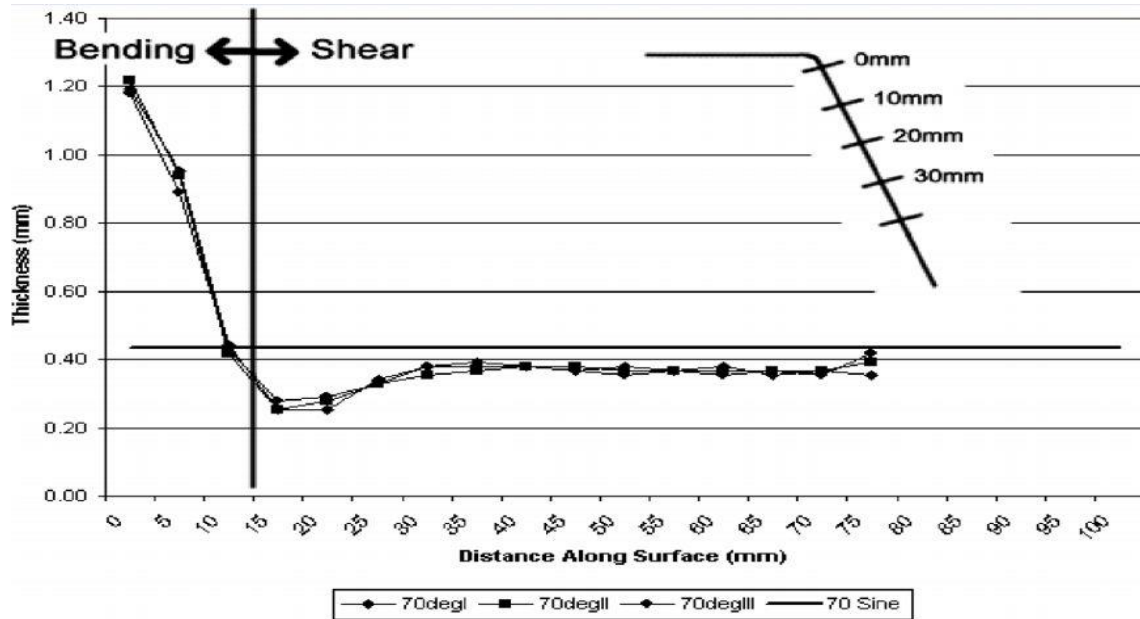


Figure 1.10: Thickness variation of a 70 degree cone formed using SPIF [9]

The thinning band in 70° cones is shown in Fig.1.11

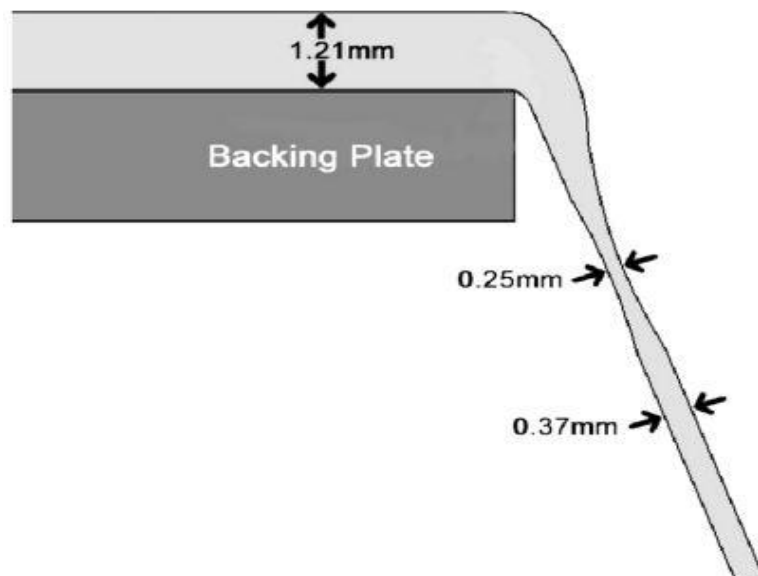


Fig 1.11 Thinning Band on 70° wall angle cone [9]

Hirt et al. [10] adopted a multistage strategy in which the component is preformed in a shallow wall angle of 45° in first stage as shown in Fig.1.12. In the following stages, they used upward and downward movement to produce the final component with an angle of about 80° as shown in Fig.1.13.

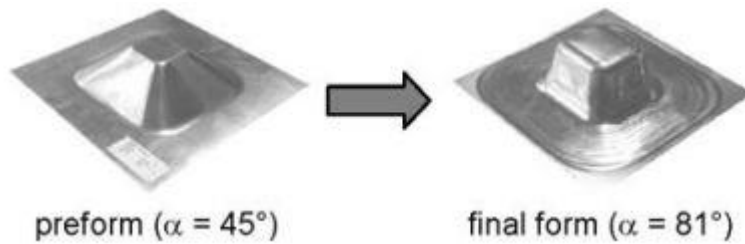


Figure 1.12: Preform and the final component [10]

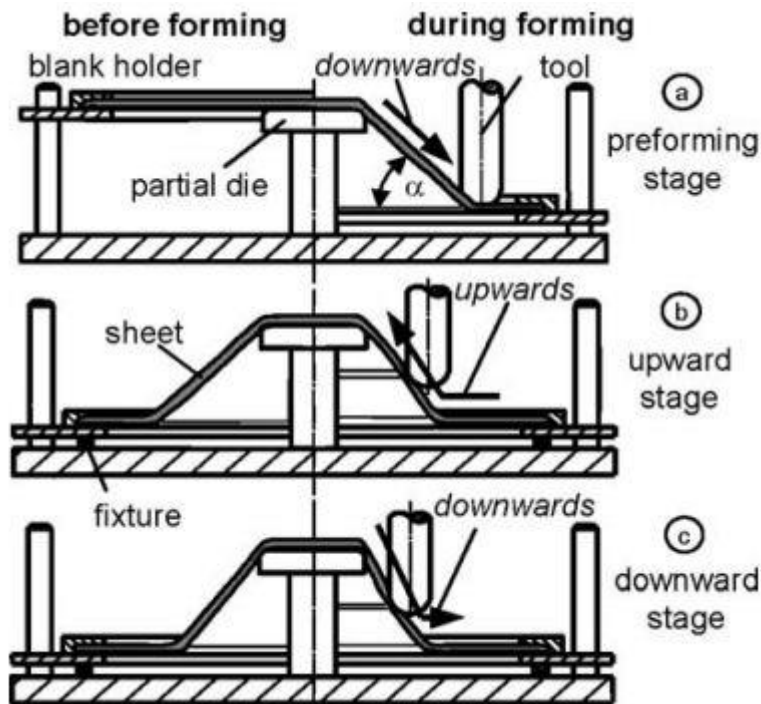


Figure 1.13: Multistage forming strategy [10]

Skjoedt et al. [11] used a five stage forming strategy for SPIF of a circular cylindrical cup with a height to radius ratio of one as shown in Fig.1.14. In the second stage, he found out the influence of forming direction. i.e, upwards or downwards. They investigated mainly two configurations viz; down-up-down-down (DUDD) and down-down-down-up (DDDU).

The DDDU strategy can be used up to fourth stage without fracture whereas the DUDD component got fractured in the 4th stage. From the above Fig. 1.15 it is evident that the DUDD component failed at the corner which is the transition zone between vertical and horizontal part. Fracture occurs at the corner where there is bi-axial stretching. The problem with the DDDU component is that the downward movement results in rigid body translations at the bottom of the component.

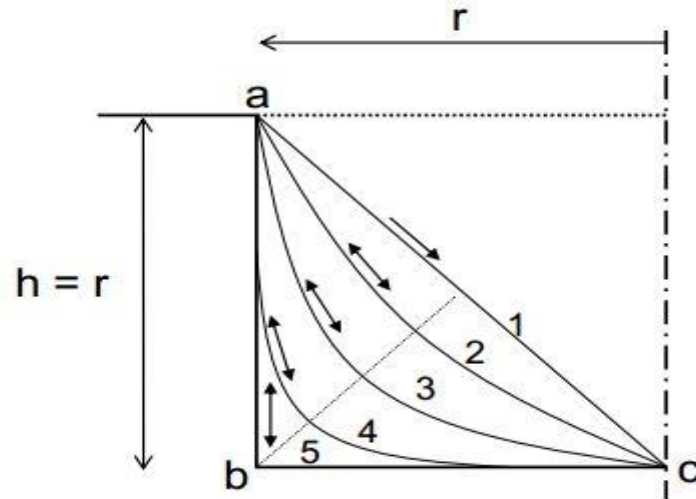


Figure 1.14: Five stage strategy for forming a cup [12]



Figure 1.15: DDDU and DUDD strategy [12]

Duflou et al. [12] stated that maximum wall angle that can be formed is a limitation of SPIF because at higher wall angles, sine law is not valid. So, to achieve higher wall angles, material redistribution has to be done by shifting the material from other zones to inclined wall areas. To achieve this, they adopted a multistage strategy which comprises of five stages to form a cylindrical part. Sine law is applicable for the first stage where the points are translated downward. But from the next stage onwards, instead of downward translation, the points are rotated which implies sine law is not valid. From the above Fig1.16 it is evident this strategy results in the accumulation of rigid body translations which eventually result in the formation of stepped features which causes the deviation of the formed geometry from the desired geometry. So tool path has to be planned in such a way that it should reduce the rigid body translations and the thinning which occurs at the corner resulting to fracture. Material redistribution has to be done by shifting the material from regions having more thickness to the wall regions having less thickness during the intermediate stages.

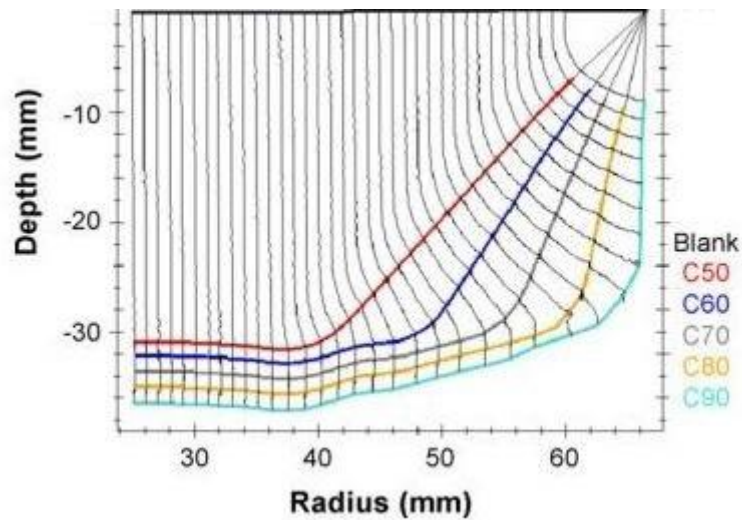


Figure 1.16: Multi pass strategy [13]

Malhotra et al. [13] used a seven stage strategy to form a cylinder by using mixed tool paths as shown in Fig.1.17. They used a combination of in-to-out and out-to-in tool paths to successfully form the cylindrical component. Some regions are not deformed during the intermediate stages keeping in consideration that those regions will move towards the corner region of the final stage where chances of failure are more due to thinning.

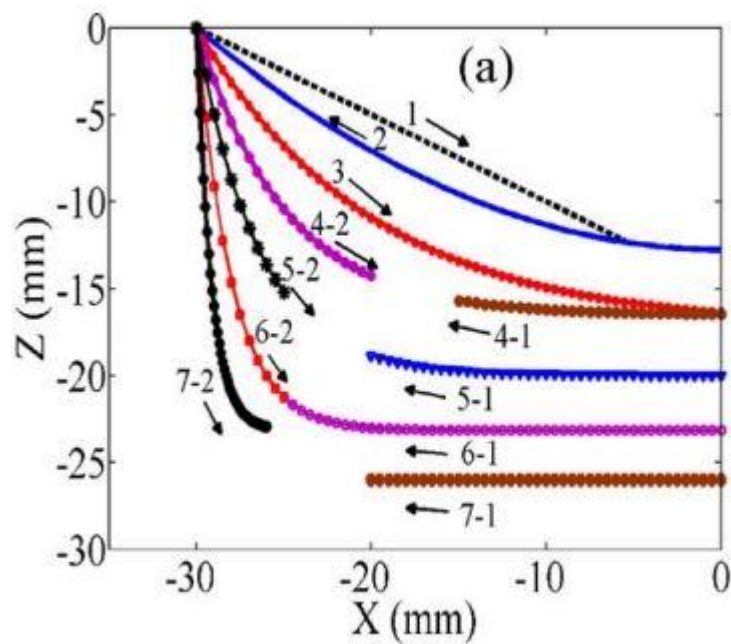


Figure 1.17: Multi-pass strategy using mixed tool paths [14]

1.3 Objective of the present work

Literature review indicates that it is impossible to form a larger wall angle component in single stage SPIF. When multistage strategy is used, it resulted in the accumulation of rigid body translations which resulted in the formation of stepped features at the bottom of the component. One method to eliminate this is to use a combination of out to in & in to out tool movement in intermediate stages. Excessive thinning of the material at the corner is another problem which can be eliminated by selectively deforming the material in intermediate stages. Malhotra et al. [14] succeeded in predicting the stepped feature formation in multi-pass single point incremental forming and formed hemispherical and ellipsoidal components with constant thickness.

Objective of present work is to calculate the rigid body translations which occurs when the tool is moved from out to in.

1.4 Organization of the thesis

A brief introduction to incremental forming has been given in this chapter followed by the literature survey. Objective of present work is also defined in this chapter.

The organization of thesis is reported as follows:

Chapter 2 presents the details regarding Toolpath planning in a multistage strategy and rigid body translation & methodology to predict thickness distribution in Multistage SPIF is also presented.

Chapter 3 presents the results and discussion based on the methodologies.

Chapter 4 concludes the report with scope for future work.

Chapter 2

Methodology

2.1 Tool Path Planning for Multistage

In multistage strategy, the intermediate stages play a significant role in determining the shape and thickness distribution of the final component,

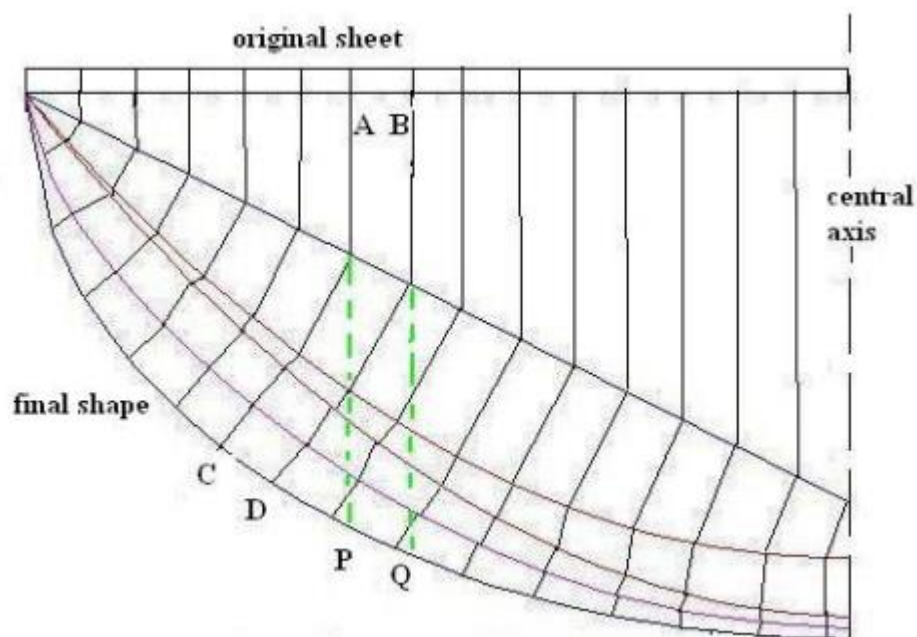


Figure 2.1: Methodology for multistage [14]

According to the methodology proposed by Abhishek [14], the point which is in the previous stage will move normally to the next stage. Normals can be drawn from former stage to latter stage. The points where the normal cut the latter stage is taken and are used for drawing further normal to the next stage. This method is continued until normals intersect the final stage as shown in Fig.2.1. Length of the deformed element is calculated by taking the consecutive intersection points. Thickness after a particular stage can be found out by applying volume constancy for each element between initial shape and final shape of element. This method of calculating holds true if tool is moved completely from out-to-in. In intermediate stages, some portion is untouched in a particular stage, then for that untouched portion of the component, previous stage thickness is used.

When the tool moves from out to in, the undeformed part moves rigidly downwards. So tool path has to be designed taking these rigid body translations into account. When in-to-out strategy is adopted, the tool should start from the last point of the previous stage and rigid body translation in this case is also different. This deviation in rigid body translation is because of the clamping of the sheet at the top.

2.1.1 Tool radius compensation

When a 3-axis CNC milling machine is used, tool tip is used as reference point to specify tool path. If tool path compensation is not given, then tool will gouge into the material. This will affect the accuracy of the formed component.

From the co-ordinates of tool contact point, tool center and tool tip points are calculated as shown in Fig.2.2

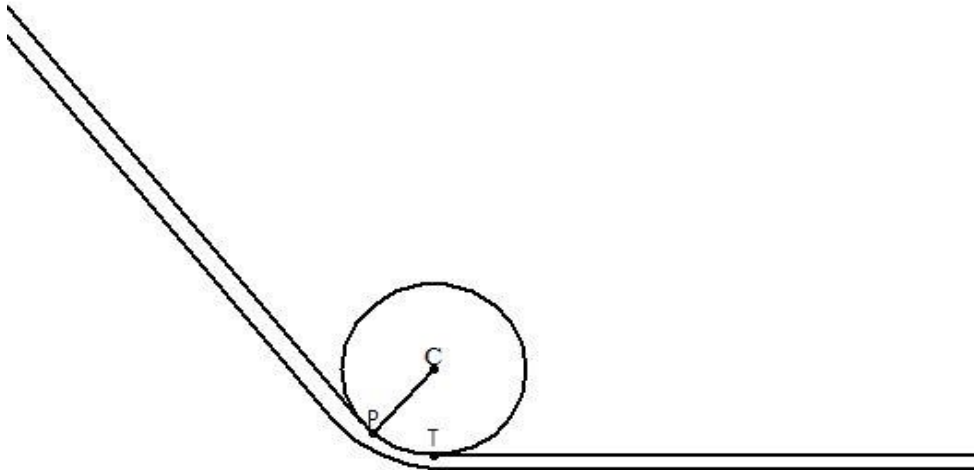


Figure 2.2: Tool radius compensation

$$\vec{C} = \vec{P} + R \cdot \hat{n}$$

$$\vec{T} = \vec{C} - R \cdot \hat{k}$$

Where R is the radius of tool

C- centre of tool

P- tool contact point

T – tool tip point

2.2 Rigid body translation

When tool moves from out-to-in, the undeformed part will move rigidly downwards. In multi-stage SPIF, due to the accumulation of rigid body translations during the intermediate stages, accuracy of the formed component is reduced and results in the formation of stepped features.

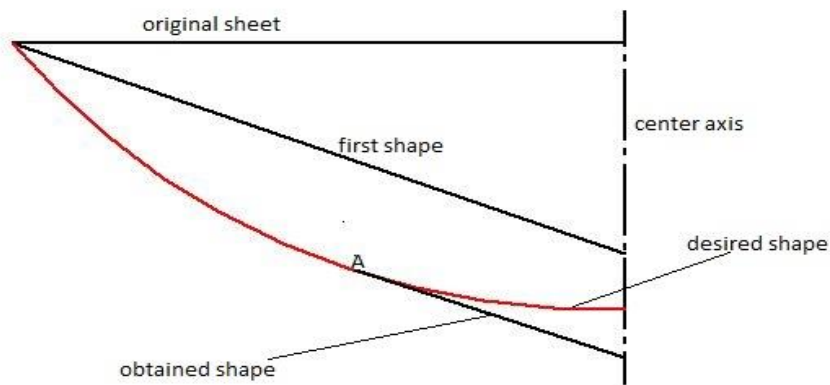


Figure 2.3: Rigid body translation

Two intermediate stages in multistage SPIF are shown in Fig.2.3. If the co-ordinates of the first stage are given to tool tip, it will result in rigid body translation. At the point of maximum displacement from the initial profile (A), the tool won't touch the work piece because the material has already been rigidly displaced which is more than the required geometry.

The methodology used for calculating rigid body translation can be explained as follows:

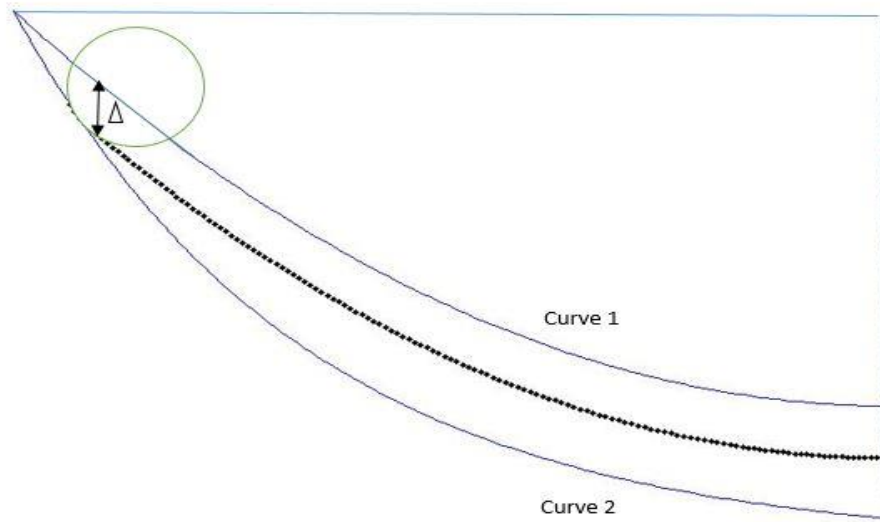
Steps

1. Tool contact points are calculated using incremental depth i.e, by dividing the depth of the component by incremental depth.
2. From tool contact point, tool centre and tool tip point are calculated.
3. Slope comparison

Tool contact leaving point can be found out by comparing the slope of a point on the curve to the slope of a point on the tool.

4. Using the depth of tool leaving point, rigid body displacement (Δ) is calculated & is represented as shown in Fig. 2.4.
5. Calculation of points of a particular contour
 - a. If the previous curve x-coordinate is less than the tool contact point x-coordinate, the corresponding co-ordinates of next stage is taken as the contour points.
 - b. If the previous curve x-coordinate lies in between the tool contact to tool contact leaving region, points on the tool geometry is taken as contour points.
 - c. If the previous curve x-coordinate is more than the tool leaving x-coordinate, rigid body displacement is added to the corresponding points on the previous curve.

6. The same procedure is repeated until required geometry is obtained.



1

Figure 2.4: Methodology for rigid body translation

Chapter 3

Results

3.1 Thickness Calculation

Before applying this methodology explained in chapter 2, one has to validate the works done on cylindrical shape by Malhotra et al. [13]. The methodology is implemented using Matlab software. Once the points on the final stage are obtained, thickness is calculated by applying volume constancy for elements using Pappus' theorem. The material movement during intermediate stages are shown in Fig.3.2

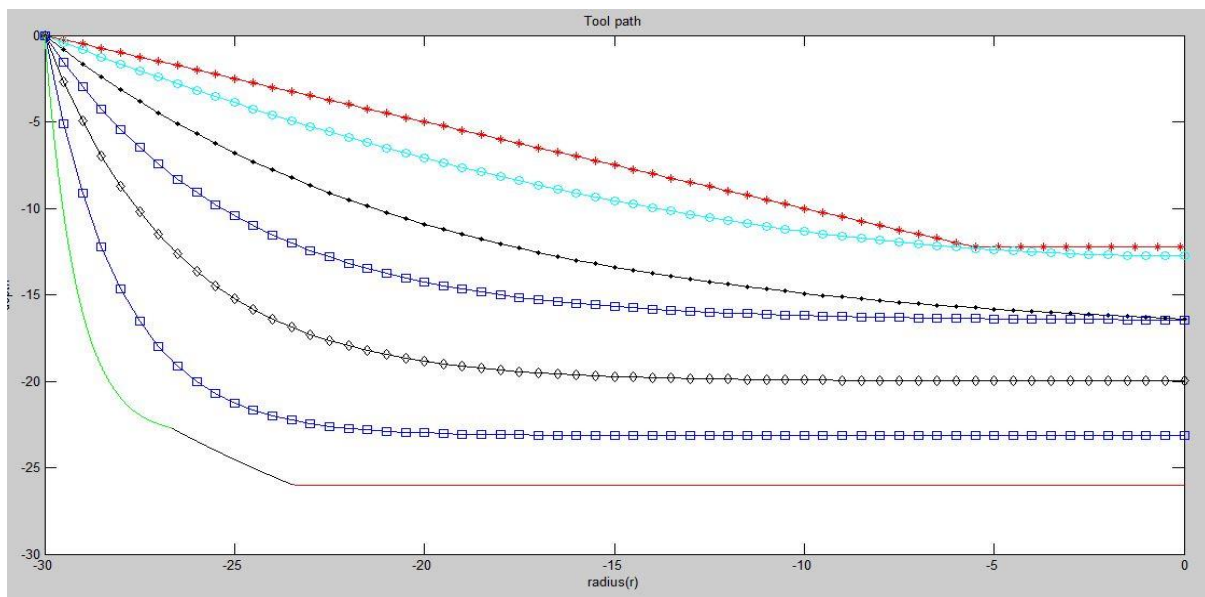


Figure 3.1: Tool path for multistage [14]

The equations for the 7 stages

Stage 1

The expression for stage 1 is given by

$$z_1 = -0.6 \frac{h}{r} (x + r), \text{ where } h=25, r=30$$

In this stage, tool is moved out-to-in from $x=-30$ to $x=-1.1 R$, where R is the radius of the tool.

Stage 2

The expression for stage 2 is given by

$$z_2 = 0.51 \frac{h}{r^2} (x^2 - 0.51h)$$

In this stage, tool is moved completely in-to-out.

Stage 3

The expression for stage 3 is given by

$$z_3 = 0.69he^{-(x+r)/10} - 0.69h$$

In this stage, tool is moved completely out-to-in from $x=-30$ to $x=0$.

Stage 4

The expression for stage 4 is given by

$$z_4 = 0.66he^{-(x+r)/5} - 0.66h$$

In this stage, first tool is moved in-to-out from $x=0$ to $x=-15$ mm and then moved out-to-in from $x=-30$ to $x=-20$. The region from $x=-15$ to $x=-20$ is undeformed.

Stage 5

The expression for stage 5 is given by

$$z_5 = 0.8he^{-(x+r)/3.5} - 0.8h$$

In this stage, first tool is moved in-to-out from $x=0$ to $x=-20$ mm and then moved out-to-in from $x=-30$ to $x=-25$.

Stage 6

The expression for stage 6 is given by

$$z_6 = 0.926he^{-(x+r)/2} - 0.926h$$

In this stage, first tool is moved in-to-out from $x=0$ to $x=-25$ mm and then moved out-to-in from $x=-30$ to $x=-25$.

Stage 7

The expression for stage 7 is given by

$$z_7 = he^{-(x+r)/10} - h$$

In this stage, first tool is moved in-to-out from $x=0$ to $x=-20$ mm and then moved out-to-in from $x=-30$ to $x=-27.5$.

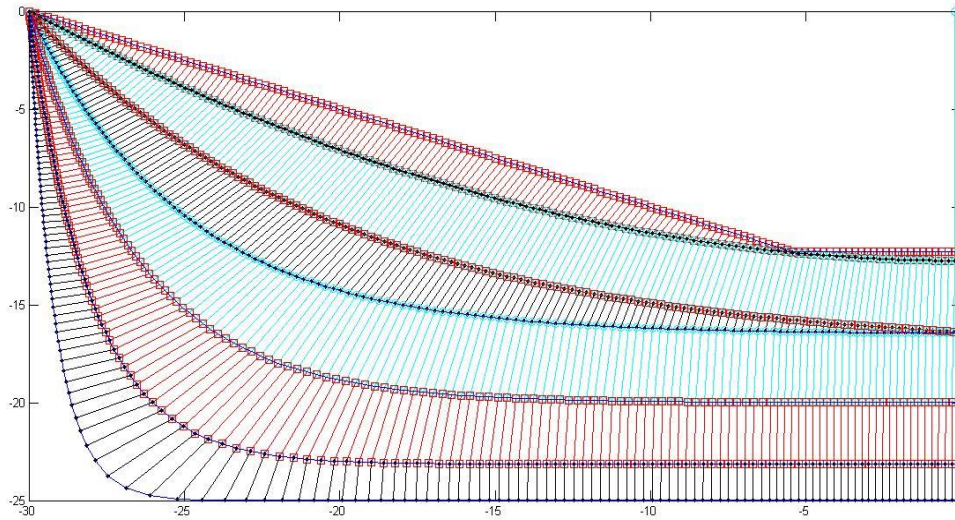
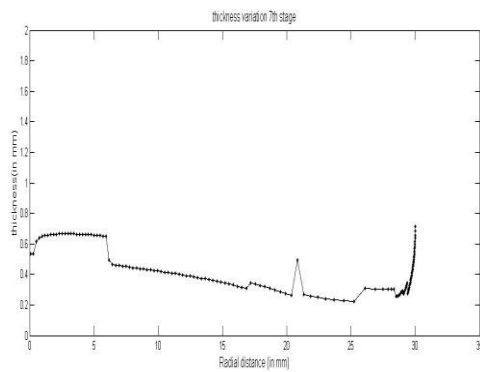


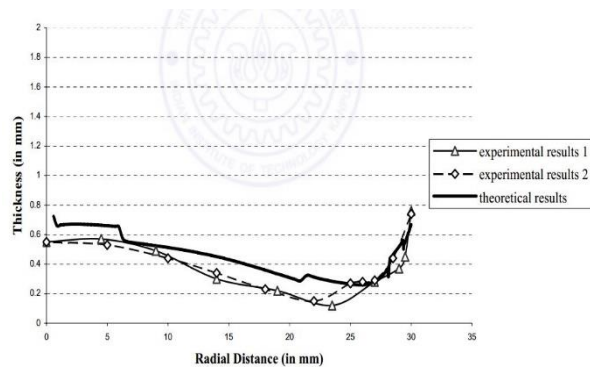
Figure 3.2: Material movement during intermediate stages

3.1.1 Thickness Variation

Thickness variation for stage 7 is shown in Fig. 3.3. From the thickness variation, it is evident that top wall region has undergone the most thinning. This can be reduced by selectively deforming the material in previous stages & by changing the out-to-in and in-to-out distances. It can be observed that the theoretical and experimental results are matching.



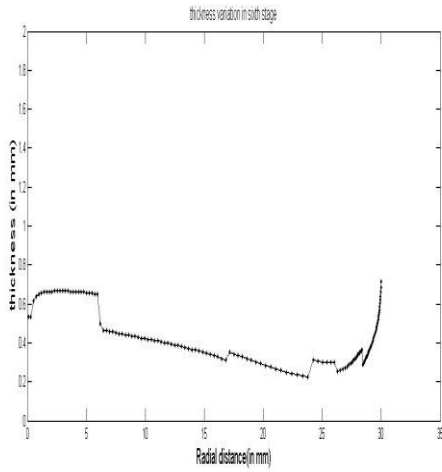
(a) Thickness variation for stage 7



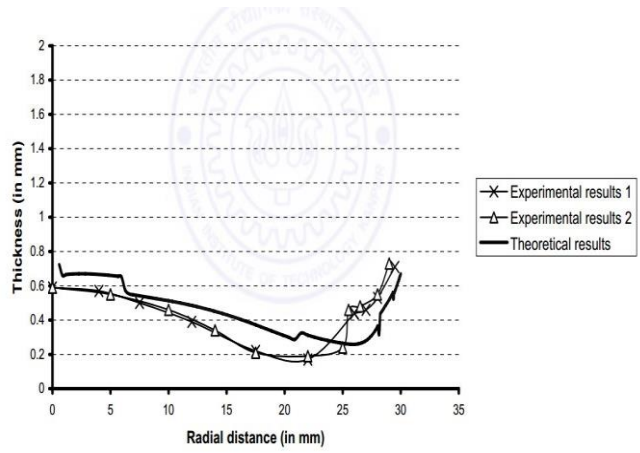
(b) Thickness variation for stage 7 [14]

Figure 3.3: Comparison of thickness variation for stage 7

Comparison of thickness variation for stage 6 is shown in Fig. 3.4. It can be observed that the theoretical and experimental results are matching.



(a) Thickness variation for stage 6



(b) Thickness variation for stage 6 [14]

Figure 3.4: Comparison of thickness variation for stage 6

Thickness variation for stages 1-5 are shown in Fig.3.5-3.9.

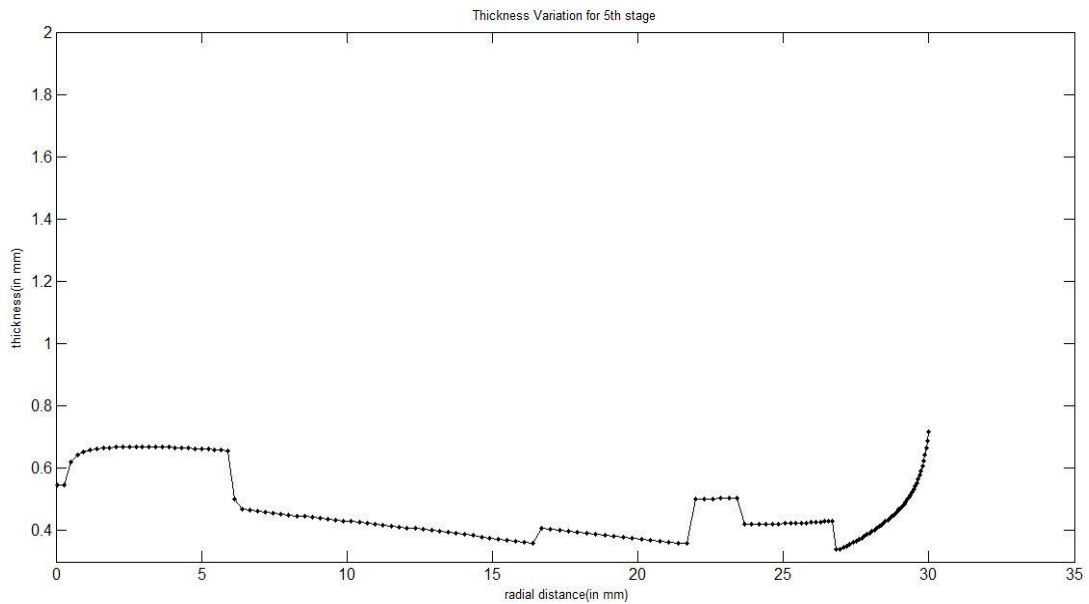


Figure 3.5: Thickness variation for stage 5

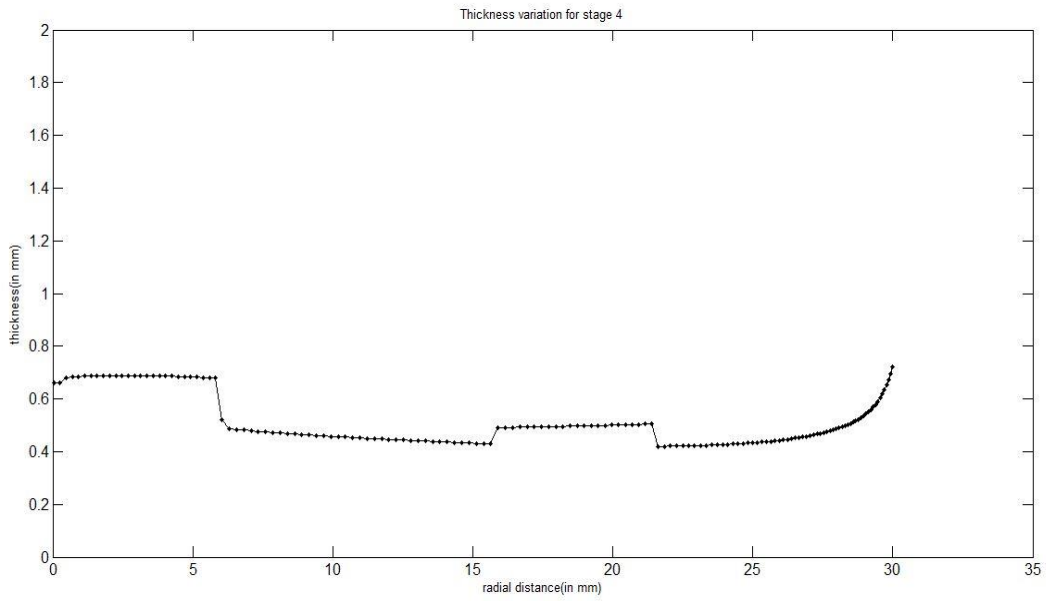


Figure 3.6: Thickness variation for stage 4

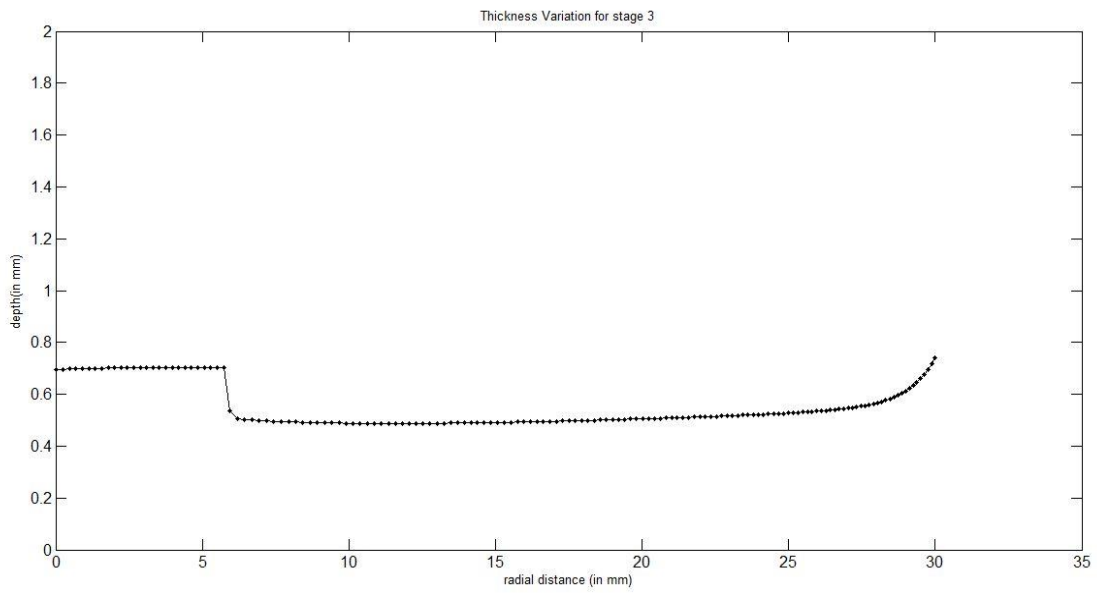


Figure 3.7: Thickness variation for stage 3

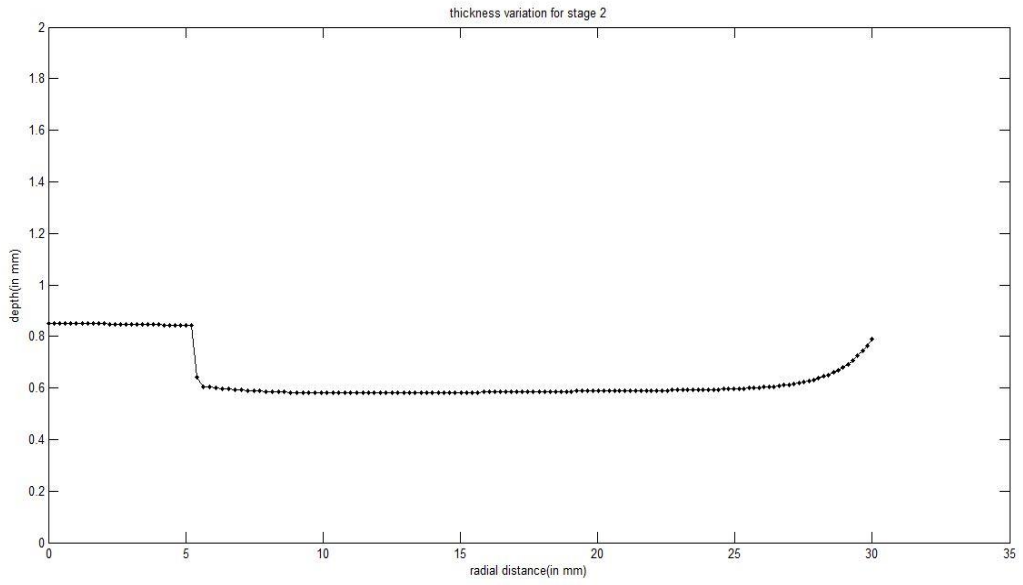


Figure 3.8: Thickness variation for stage 2

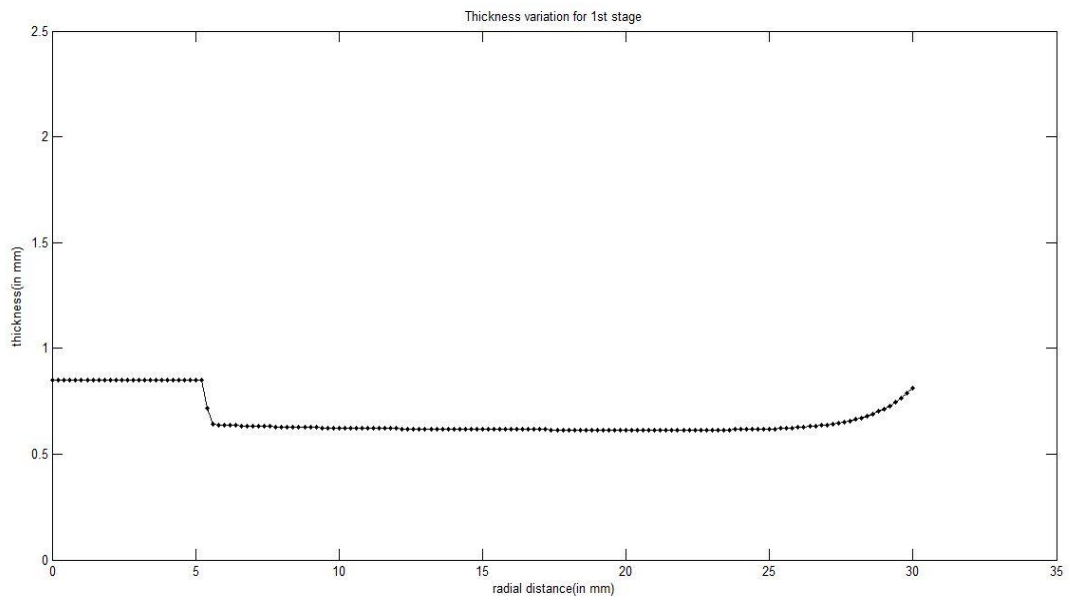


Figure 3.9: Thickness variation for stage 1

3.2 Rigid body translation

Rigid body translation for out-to-in profiles are calculated using the methodology used in chapter 2.

Stage1: The expression for this stage is given by

$$z_1 = -0.6 \frac{h}{r} (x + r) \text{ Where } h \text{ is the height of the cylinder and } r \text{ is the radius of cylinder}$$

$$H=25, r=30;$$

In this stage tool is moved out-to-in from $x=-30$ to $x=0$. The rigid body movement is shown in Fig.3.10. The dotted lines show the profile after each contour after accounting rigid body translation. The black dots show the tool contact region.

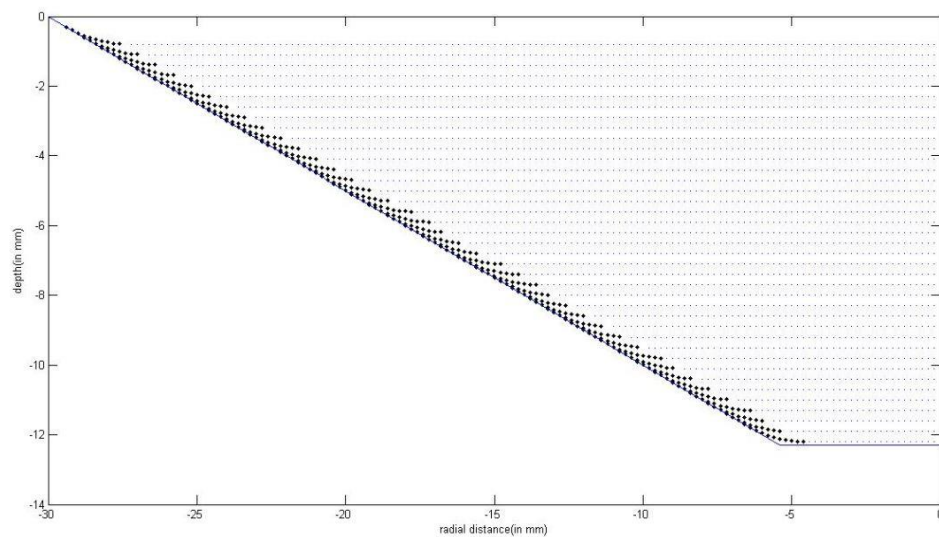


Figure 3.10: Rigid body translation for stage 1

Stage3: The expression for this stage is given by

$$z_3 = 0.69he^{-(x+r)/10} - 0.69h.$$

The previous stage expression is given by

$$z_2 = 0.51 \frac{h}{r^2} (x^2 - 0.51h) \text{ Where } h \text{ is the height of the cylinder and } r \text{ is the radius of cylinder}$$

$$H=25, r=30;$$

In this stage tool is moved out-to-in from $x=-30$ to $x=0$. The profiles are shown in Fig.3.11. The rigid body movement is shown in Fig.3.12. The dotted lines show the profile after each contour after accounting rigid body translation. The black dots shows the tool contact region at each contact point.

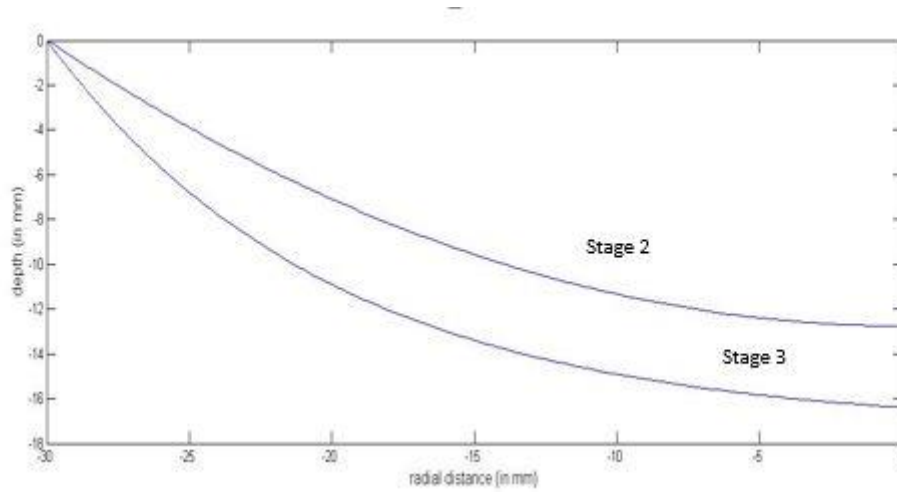


Figure 3.11: Resultant shapes after stage 2 and 3

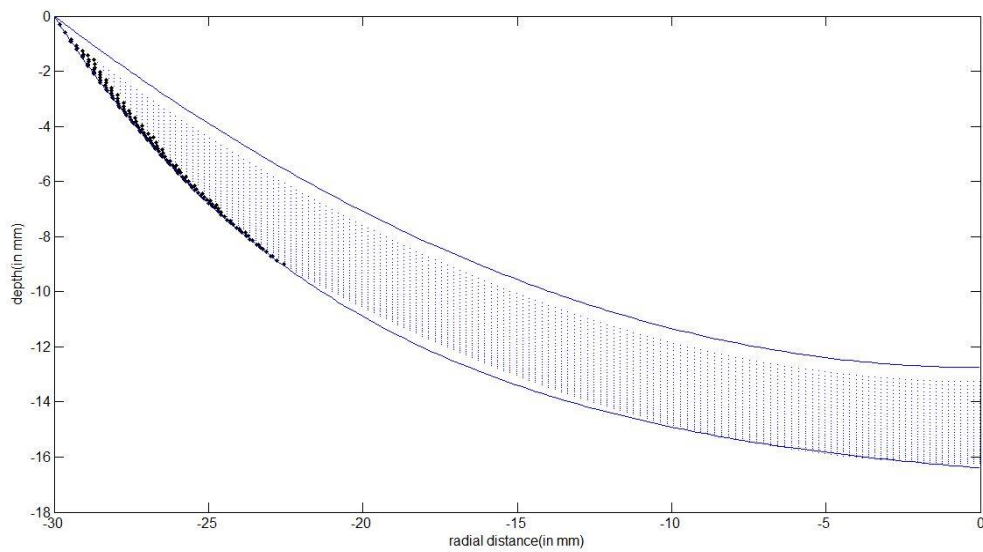


Figure 3.12: Rigid body translation for stage 3

Stage5: the expression for this stage is given by

$$z_5 = 0.8he^{-(x+r)/3.5} - 0.8h$$

The previous stage expression is given by

$$z_4 = 0.66he^{-(x+r)/5} - 0.66h$$

In this stage tool is moved out-to-in from $x = -30$ to $x = -25$. The profiles are shown in Fig.3.13. The rigid body movement is shown in Fig.3.14. The dotted lines show the profile after each contour after accounting rigid body translation.

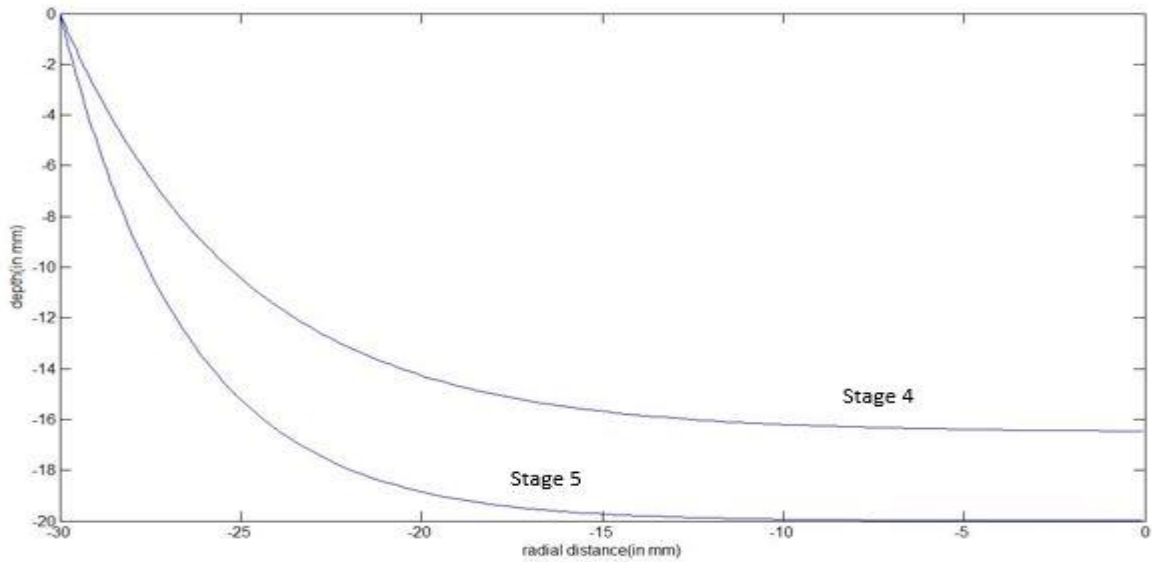


Figure 3.13: Resultant shapes after stage 4 and 5

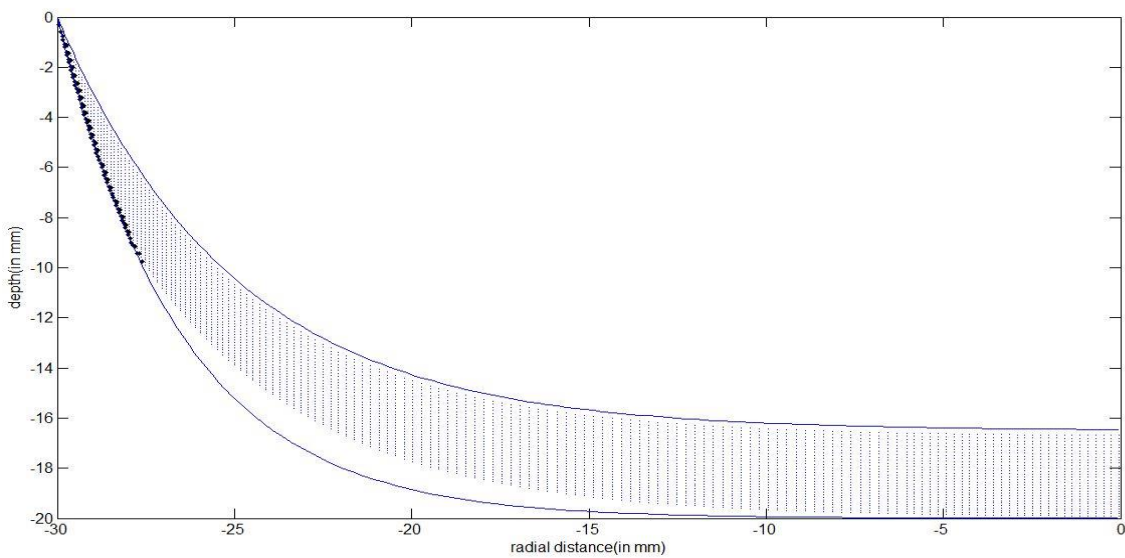


Figure 3.14: Rigid body translation for stage 5

Stage6: the expression for this stage is given by

$$z_6 = 0.926he^{-(x+r)/2} - 0.926h$$

The previous stage expression is given by

$$z_5 = 0.8he^{-(x+r)/3.5} - 0.8h$$

In this stage tool is moved out-to-in from $x = -30$ to $x = -25$. The profiles are shown in Fig.3.15. The rigid body movement is shown in Fig.3.16. The dotted lines show the profile after each contour after accounting rigid body translation.

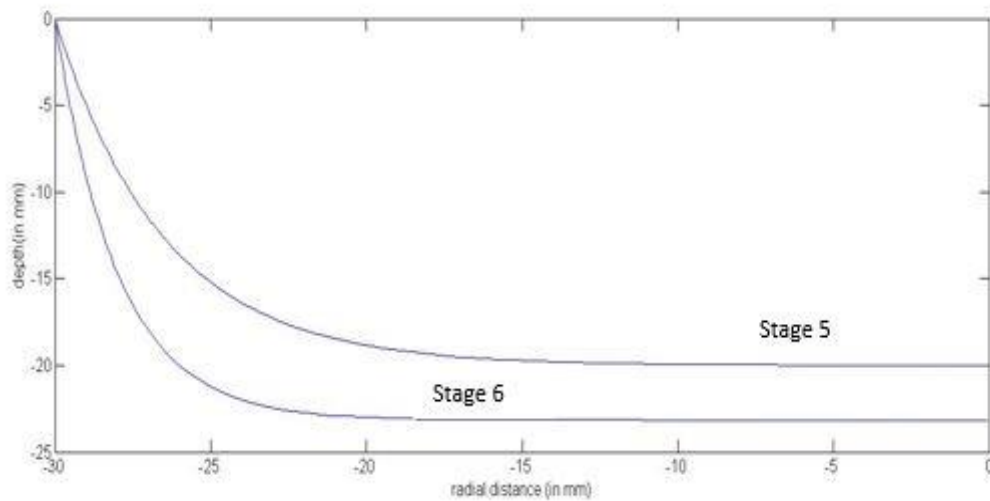


Figure 3.15: Resultant shapes after stage 5 and 6

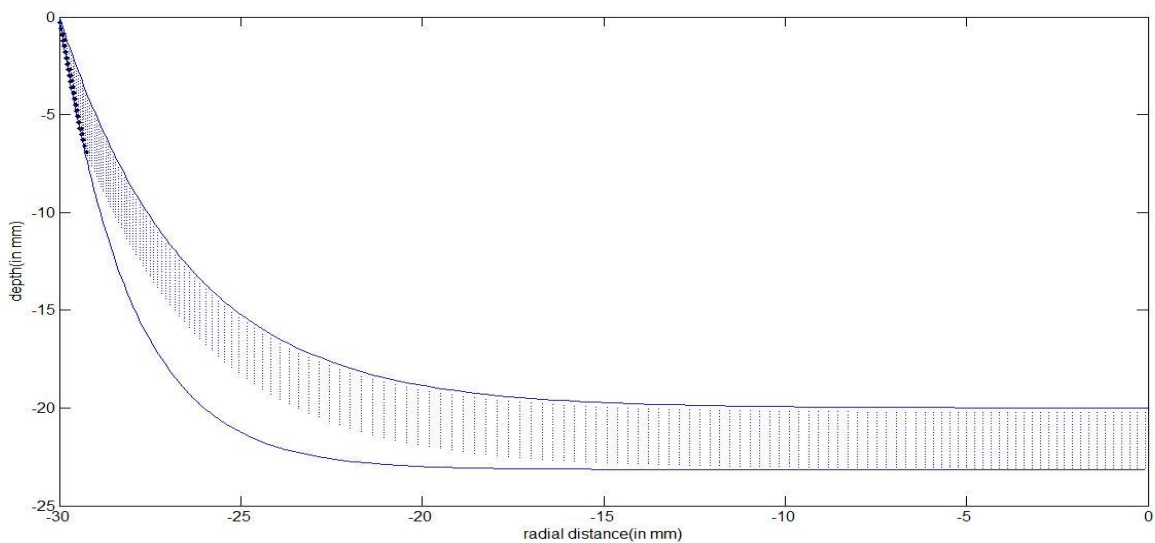


Figure 3.16: Rigid body translation for stage 6

Stage7: the expression for this stage is given by

$$z_7 = he^{-(x+r)/0.85} - h$$

The previous stage expression is given by

$$z_6 = 0.926he^{-(x+r)/2} - 0.926h$$

In this stage tool is moved out-to-in from $x = -30$ to $x = -27.5$. The profiles are shown in fig. 3.17. The rigid body movement is shown in Fig.3.18. The dotted lines show the profile after each contour after accounting rigid body translation.

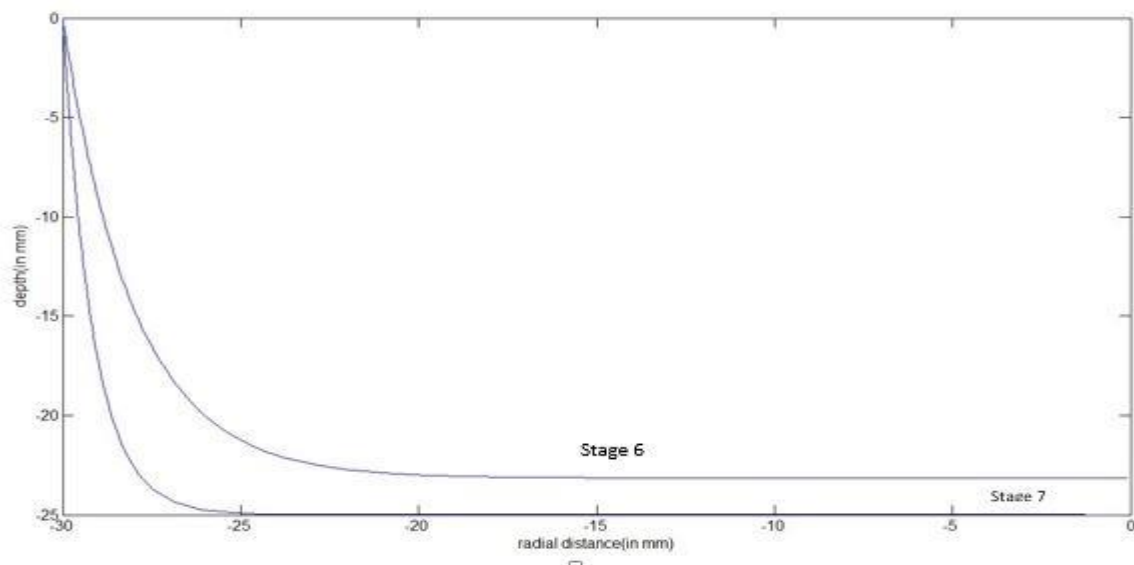


Figure 3.17 Resultant shapes after stage 6 and 7

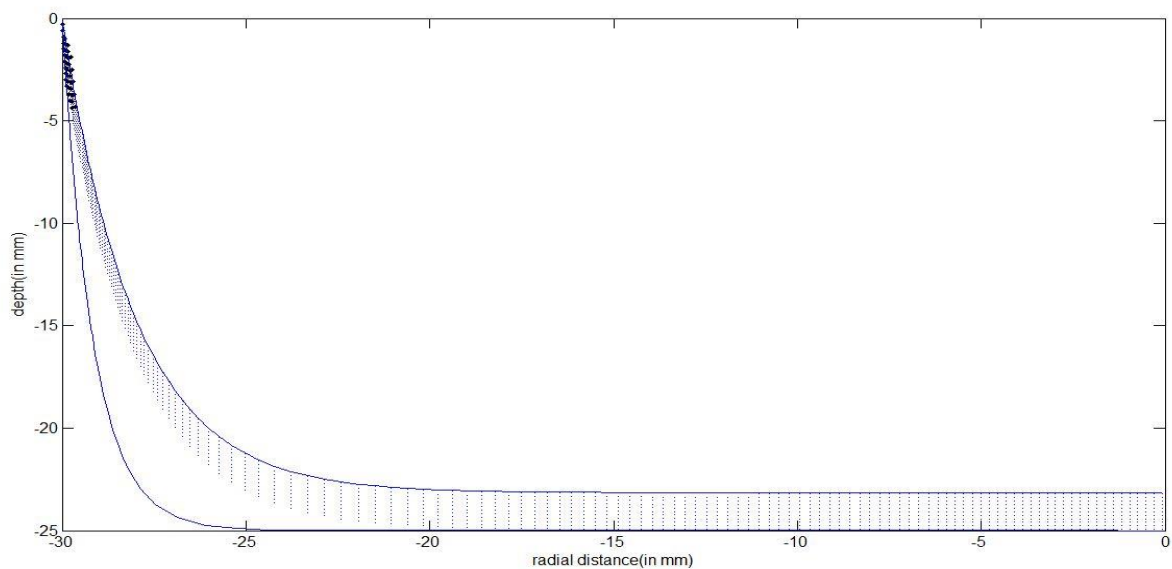


Figure 3.18: Rigid body translation for stage 7

Chapter 4

Conclusions and Scope for future work

4.1 Conclusions

- Validation of the work has been done and thickness variation has been calculated by the proposed methodology.
- In multi stage even though the larger wall component has been made, but thickness variation is not uniform.
- Top wall region is undergoing the most thinning. This is due to the variations in rigid body translations and the selection of the tool movement direction.
- Excessive thinning of the material at the corner is eliminated by selectively deforming the material in intermediate stages.
- Rigid body translation is calculated for out-to-in tool paths. This can be used to improve the accuracy of the component formed.

4.2 Scope for future work

- Rigid body translation for in-to-out tool paths can be calculated.
- By using a combination of out-to-in and in-to-out tool paths, components can be formed with more accuracy.

REFERENCES

- [1] Martins P. A. F., Bay N., Skjoedt M., and Silva M. B., 2008, "Theory of single point incremental forming," *CIRP Annals - Manufacturing Technology*, **57**(1), pp. 247–252.
- [2] Cao, J., Huang, Y., Reddy, N. V., Malhotra, R., and Wang, Y., 2008, "Incremental Sheet Metal Forming: Advances and Challenges," International Conference on Technology of Plasticity (ICTP – 2008), September 7–11, Gyeongju, South Korea.
- [3] Shim M.-S., and Park J.-J., 2001, "The formability of aluminium sheet in incremental forming," *Journal of Materials Processing Technology*, **113**(1–3), pp. 654–658.
- [4] Kim T. J., and Yang D. Y., 2000, "Improvement of formability for the incremental sheet metal forming process," *International Journal of Mechanical Sciences*, **42**(7), pp. 1271–1286.
- [5] Silva M. B., Skjoedt M., Martins P. A. F., and Bay N., 2008, "Revisiting the fundamentals of single point incremental forming by means of membrane analysis," *International Journal of Machine Tools and Manufacture*, **48**(1), pp. 73–83
- [6] Filice L., Fratini L., and Micari F., 2002, "Analysis of Material Formability in Incremental Forming," *CIRP Annals - Manufacturing Technology*, **51**(1), pp. 199–202.
- [7] Duflou J., Tunçkol Y., Szekeres A., and Vanherck P., 2007, "Experimental study on force measurements for single point incremental forming," *Journal of Materials Processing Technology*, **189**(1–3), pp. 65–72.
- [8] Jackson K., and Allwood J., 2009, "The mechanics of incremental sheet forming," *Journal of Materials Processing Technology*, **209**(3), pp. 1158–1174.
- [9] Young D., and Jeswiet J., 2004, "Wall thickness variations in single-point incremental forming," *Proceedings of the Institution of Mechanical Engineers, Part B: Journal of Engineering Manufacture*, **218**(11), pp. 1453–1459.
- [10] Hirt G., Ames J., Bambach M., Kopp R., and Kopp R., 2004, "Forming strategies and Process Modelling for CNC Incremental Sheet Forming," *CIRP Annals - Manufacturing Technology*, **53**(1), pp. 203–206.
- [11] Skjoedt M., Bay N., Endelt B., and Ingarao G., 2008, "Multi Stage Strategies for Single Point Incremental Forming of a Cup," *Int J Mater Form*, **1**(1), pp. 1199–1202.
- [12] Duflou J. R., Verbert J., Belkassam B., Gu J., Sol H., Henrard C., and Habraken A. M., 2008, "Process window enhancement for single point incremental forming through multi-step tool paths," *CIRP Annals - Manufacturing Technology*, **57**(1), pp. 253–256.
- [13] Malhotra R., Bhattacharya A., Kumar A., Reddy N. V., and Cao J., 2011, "A new methodology for multi-pass single point incremental forming with mixed toolpaths," *CIRP Annals - Manufacturing Technology*, **60**(1), pp. 323–326.
- [14] Abhishek K., 2009, "Multi-stage Tool path Strategies for Single-Point Incremental Forming," M.Tech. Thesis, IIT Kanpur.
- [15] Shubin E., 2012, "Finite Element Analysis of Incremental Sheet Metal Forming", M.Tech. Thesis, IIT Kanpur.

APPENDIX A

A.1 Experimental Setup

The experimental setup is a 3 axis 2 spindle CNC machine built at IIT Kanpur. The machine has two forming tools on either sides of the clamping platform. Sheet is clamped in between top and bottom clamping plates. Degrees of freedom of top and bottom tools are shown in Fig A-1. Machine is controlled by Siemens 840D controller which is capable of controlling top and bottom tool independently. Engine oil SAE 30 is used as lubricant and is applied on both sides of the sheet.

A.1.1 Specifications of the machine

Controller : 840D Siemens TM

Motor torque : 3 N-m for X1, X2

3 N-m for Y1, Y2

6 N-m for Z1, Z2

Spindle rpm : 1-1500

Feed : 5000 mm/min

Stroke length: 150 mm for both the tools in X, Y, Z direction

The clamping plate used is having size 95x95 mm.

Spherical ball ended tool of diameter 9.5 is used for experiments.

Models are generated using SOLIDWORKS & STEP file is used as an input format for component geometry. Top tool path is generated by applying radius compensation on tool contact points. Bottom tool path is generated by taking in account the effect of sine law & radius compensation. Tool & sheet deflections are calculated for getting compensated spiral tool path. Feed is calculated for bottom tool. Offset solid part has been generated in SOLIDWORKS. Uniform slicing method is used for slicing thicknesses of 0.1, 0.2, and 0.05 mm respectively. Adaptive slicing has been used for scallop heights of 0.001, 0.002, 0.003, 0.005, 0.0005, and 0.0064. The component which is formed by taking $dz=0,2$ is shown in Fig.A-3 & Fig.A-4. The component which is formed by taking $dz=0,1$ is shown in Fig.A-5 & Fig.A-6.



Figure A-1: ISMF machine

A 1.2 Work zero setting

1.2.1 Top tool work zero setting

Top tool is brought to the center of the clamping sheet to define the origin and z1 is set zero by touching the tool tip on top of the sheet.

1.2.2 Bottom tool work zero setting

Sheet is removed and the bottom tool is brought below the top tool zero and is made to coincide with the axis of the top tool. Work zero setting is shown in Fig.A-2.

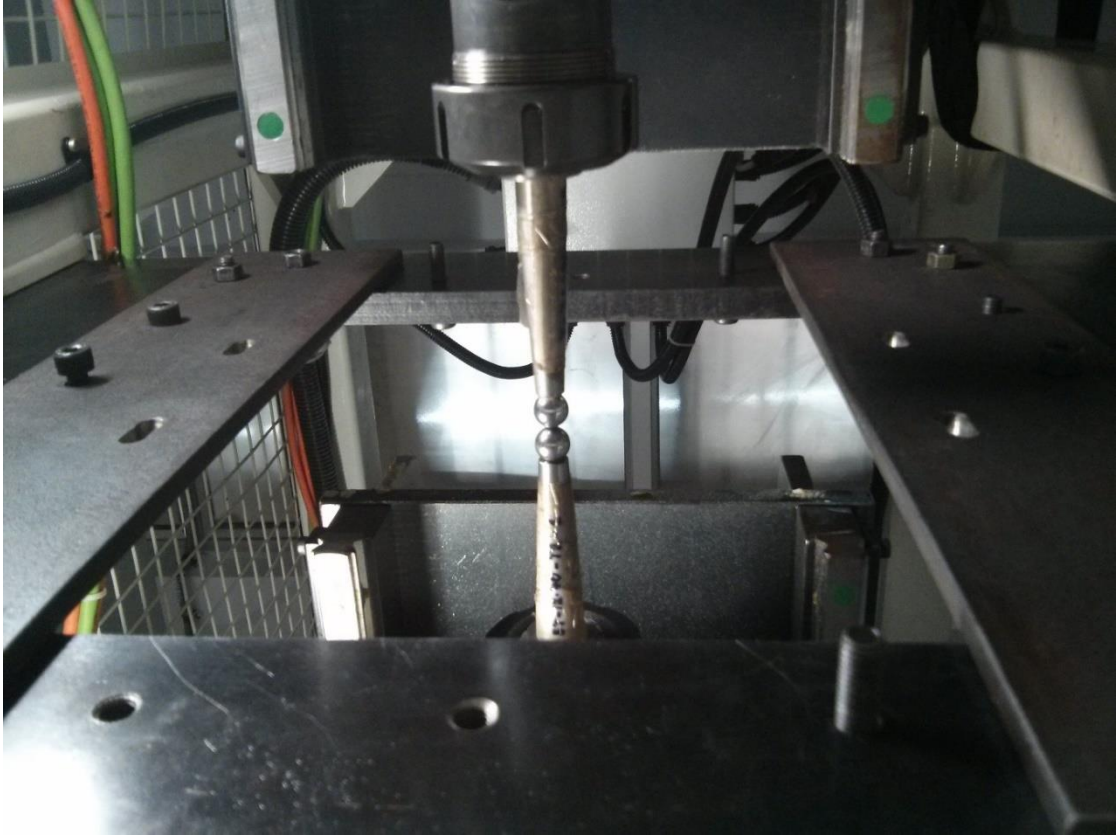


Figure A-2: Work zero setting

A 1.3 Clamping Plates

The clamping device used consists of two dimensionally identical plates; one the base plate to support the sheet and the other clamping plate to clamp it. Both the plates are made of mild steel. Clamping plate has an opening area of 95mm x 95 mm.



Figure A-3: SPIF $dz = 0.2$ component



Figure A-4: SPIF $dz = 0.2$



Figure A-5: SPIF $dz = 0.1$



Figure A-6: SPIF $dz = 0.1$

A.2 FEM (Post processing) analysis

FEM analysis (Post processing) is used for analyzing the deformation zone of SPIF cone component. Post processing of a FEA model developed by Shibin[15] has been done. The FEA model has been developed using ABAQUS to simulate SPIF. Tool is modeled as analytically rigid body. Tool tip is defined as the reference point to give boundary conditions. Sheet is modeled as deformable part with dimension 100 x 100 mm and having thickness of 0.88mm. The deformable blank & rigid tool are shown in Fig. A-7.

The material used is Al 5052. For elastic behaviour, Young's modulus (70GPa) and poissons ratio of 0.33. The plastic behaviour of sheet is given by the strain hardening law ,

$$\sigma = 385.7(\epsilon_p + 0.0089)^{0.1474}$$

For meshing, linear shell elements with enhanced hourglass control. Tool surface is chosen as the master surface and sheet top surface as the slave surface.

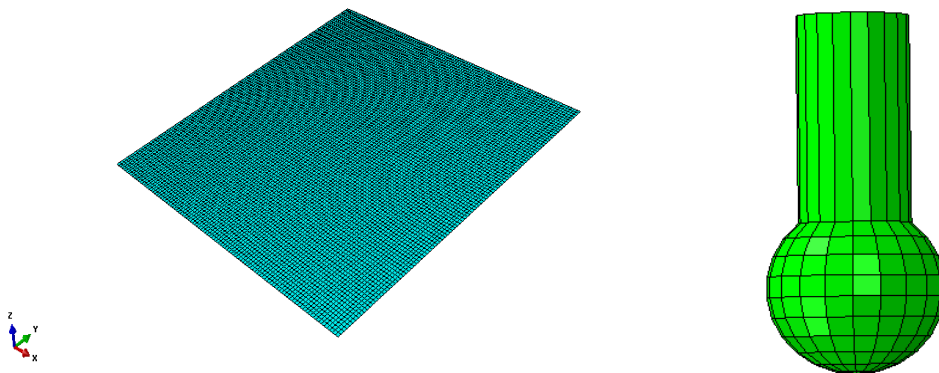


Figure A-7: Deformable blank & rigid tool in SPIF

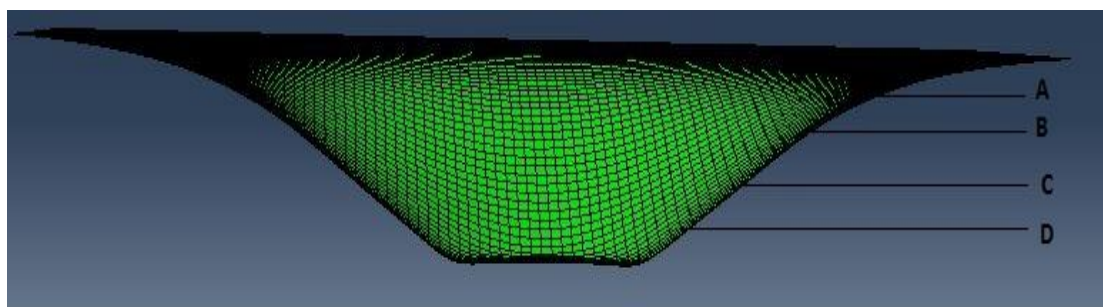
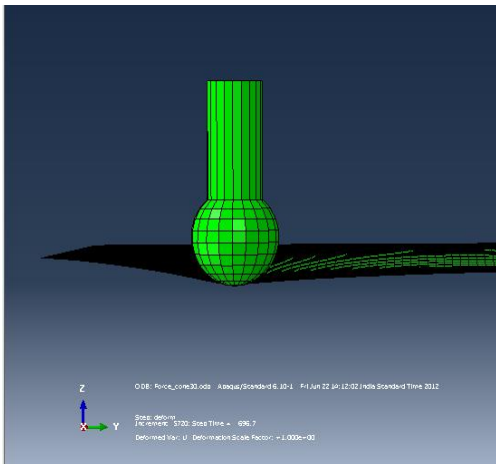


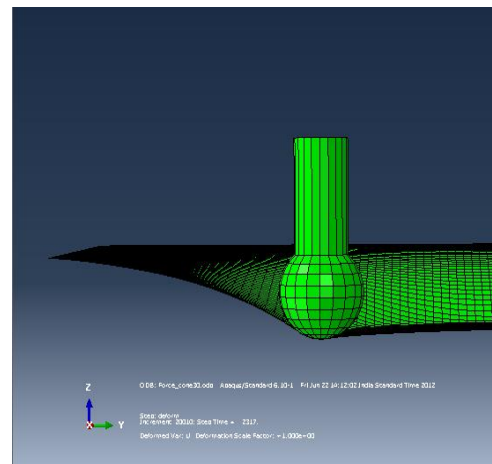
Figure A-8 Selected regions along meridional line

Deformation mechanism has been analyzed on four different regions along a meridional line as shown in Fig. A-8. The deformed regions are shown in Fig.A-9.

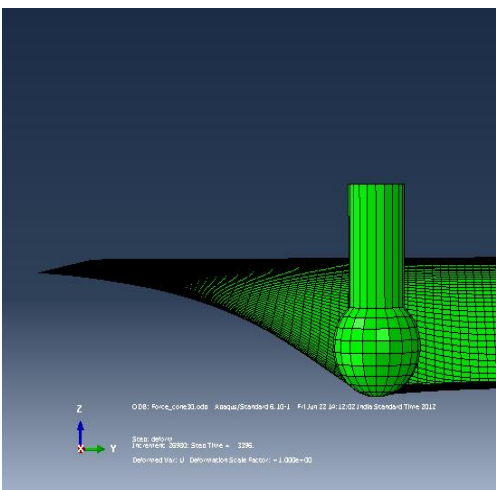
- (a) Region A (opening region)
- (b) Region B (top wall region)
- (c) Region C (bottom wall region)
- (d) Region D (near base)



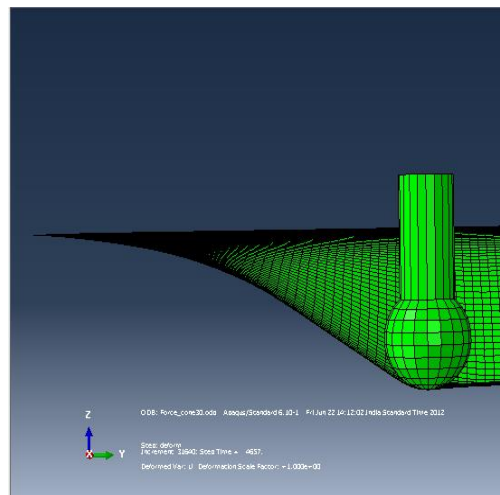
(a) Region A



(b) Region B

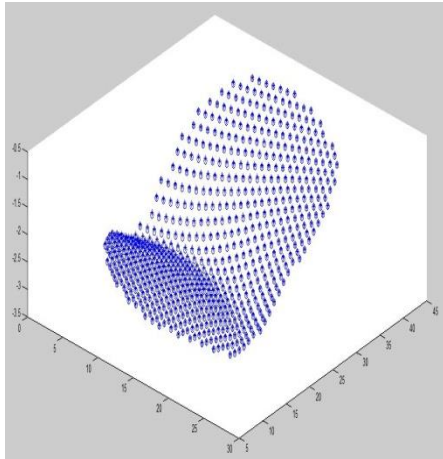


(c) Region C

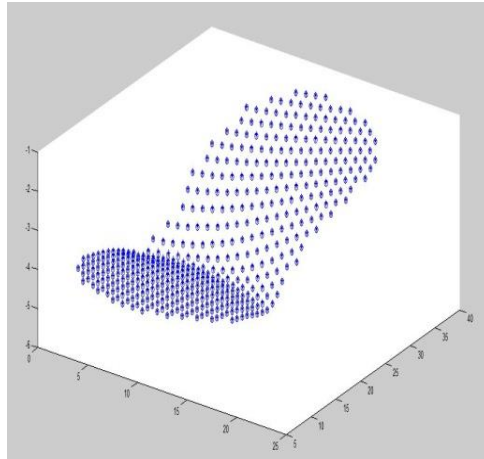


(d) Region D

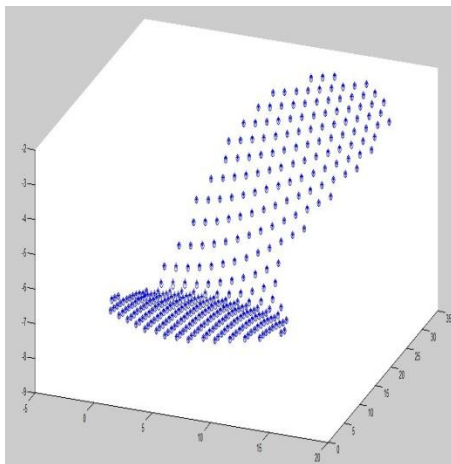
Figure A-9: Deformation at different regions in a meridional line



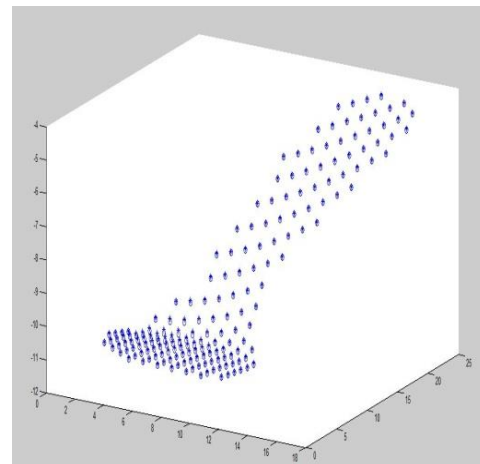
(a) Opening region



(b) Top wall region



(c) Bottom wall region



(d) near base region

Figure A-10: Displacement fields along different regions in a meridional line

In a particular time frame, the region near the tool tip will have more displacement than that of other regions. So the region which is having more displacement have to found out. The procedure can be explained as follows:

1. For a particular time frame, displacement for each node is obtained.
2. The node which is having maximum displacement is found out.
3. The nodes which are having displacement less than 20% of maximum displacement are neglected. In this way, the effective nodes around the tool contact region can be found out.

This procedure is repeated for other regions as mentioned in Fig. A-8 and the effective nodes are calculated. Table A-1 shows the number of effective nodes in different regions on a meridional line.

Region	Step Frame	ΔR	No: of effective nodes
Opening	780-781	0.08872	732
Top Wall	1276-1277	0.019646	488
Bottom Wall	1966-1967	0.027495	359
Near Base	2676-2677	0.143282	180

Table A-1: Details of finding effective nodes

Post processing has been done to visualize the deformation zone and the following observations were made:

- After analyzing different regions on meridional line, it is evident that V_{θ} (velocity along the θ direction) is having little effect on deformation zone.
- V_r (velocity in radial direction of spherical tool) is having most influence on deformation zone.
- V_{ϕ} (velocity along ϕ direction) is having very negligible effect on deformation zone.